

Galaxy Structures and External Perturbations in Gravitational Lenses

Yozo KAWANO,¹ Masamune OGURI,² Takahiko MATSUBARA,¹ and Satoru IKEUCHI¹

¹*Department of Physics and Astrophysics, Nagoya University, Chikusa-ku, Nagoya 464-8062*

kawano@a.phys.nagoya-u.ac.jp

²*Department of Physics, School of Science, The University of Tokyo, Bunkyo-ku, Tokyo 113-0033*

(Received 2003 December 17; accepted 2004 February 12)

Abstract

In modeling strong gravitational lens systems, one often adopts simple models, such as singular isothermal elliptical density plus lowest-order external perturbation. However, such simple models may mislead us if the real mass distribution is more complicated than that in the assumed models. In particular, assumptions on mass models are crucial in studying flux ratio anomalies that have been suggested as evidence for a cold dark-matter substructure. We reinvestigated four quadruple lens systems using power-law Fourier models, which have advantages of clear physical meanings and the applicability of a linear method, as well as a simple singular isothermal elliptical density model. We also investigated the effect of external perturbations, including a singular isothermal sphere, lowest-order expansion, and next-order expansion. We have found that the $\cos 3\theta$ terms of the primary galaxy and/or of external perturbation significantly reduce the χ^2 in PG 1115+080 and B1422+231. In particular, we could reproduce the flux ratios of B1422+231 with next-order external perturbation assuming 5% flux uncertainties, suggesting that external perturbation cannot be described by a simple singular isothermal sphere approximation. On the other hand, we could not fit B0712+472 and B2045+265 very well even with our models, although the χ^2 were reduced compared with the case of using simple models. Our results clearly demonstrate that both the primary lens galaxy and the external perturbation are often more complicated than we usually assume.

Key words: cosmology: dark mater — cosmology: theory — galaxies: structure — gravitational lensing

1. Introduction

Gravitational lenses of distant quasars are quite useful in cosmological and astrophysical studies, such as measuring the Hubble constant from time delays (Refsdal 1964), studies of galaxy formation and evolution, and direct probes of galaxy structure, including cold dark-matter substructures. The method used to measure the Hubble constant does not rely on the distance ladder, which inevitably suffers various systematic errors. After the discovery of the first lens system, Q 0957+561 (Walsh et al. 1979), many lens systems have been studied in detail, adopting various lens models. However, the model uncertainties, including several intrinsic degeneracies (Falco et al. 1985; Gorenstein et al. 1988; Saha 2000), prevent us from accurately deriving the Hubble constant (e.g., Wambsganss, Paczyński 1994; Keeton et al. 1997; Keeton, Kochanek 1997; Courbin et al. 1997; Wucknitz, Refsdal 1999; Witt et al. 2000; Chiba, Takahashi 2002; Wucknitz 2002; Oguri et al. 2002; Oguri, Kawano 2003).

Among several applications of gravitational lenses, flux-ratio anomalies have attracted much attention. There are mainly three explanations for them: effects of the interstellar medium, problems in smooth models, and lensing by the substructure (e.g., Kochanek, Dalal 2003). While substructure lensing is often regarded as being the best explanation for the flux anomalies (e.g., Mao, Schneider 1998; Chiba 2002), the former two explanations have not yet been sufficiently investigated to reach the conclusion that the flux-ratio anomalies are connected with the substructure. The limitation comes from the fact that it is difficult to apply all of the models, which are physical and complicated, to the observed lens systems. In addition, since galaxies are believed to consist of not only luminous matter, but also dark matter, the shapes of lens galaxies do not have to be elliptical, nor other simple shapes, as the isophotes indicate. Therefore, it is of great importance to investigate the contribution of many forms of the angular structure of the lens potential to find the true origin of the flux anomalies. Indeed, Evans and Witt (2003) showed that some of lens systems that have been claimed to be lenses with flux anomalies can be well fitted by a smooth lens model using a power-law Fourier potential (see also Oguri, Kawano 2003). Kochanek and Dalal (2003) studied the contribution of only the isothermal $m = 3$ and $m = 4$ multipoles to the flux ratio anomalies reported so far. We then reinvestigated some of the systems with not only multipoles, but also several types of external perturbations.

Our aim in this paper is to discuss the contribution of both multipoles of the primary lens galaxy and external perturbation of the group, in particular the $\cos 3\theta$ terms that are not usually included in lens modeling. We consider whether some multipoles can produce an acceptable fit without substructure or not. We also discuss the quadruple lens system B0712+472 in detail because of the interesting observations that the ellipticity of the galaxy and the shear of the group seem to be significantly misaligned ($\sim 90^\circ$) to each other, and that previous authors estimated the shear to be small compared to observations using the one-shear model (Jackson et al. 1998; Fassnacht, Lubin 2002). Since more than three images are necessary to constrain the mass models strongly, we restrict our considerations to four quadruple lens systems (PG 1115+080, B1422+231, B0712+472,

and B2045+265). There are three reasons for this restriction. First, the existence of a substructure of the lens systems has been claimed to account for the observed flux ratios (e.g., Kochanek, Dalal 2003). Second, there are no satellite galaxies that complicate the lens model. Third, there are sufficient astrometric, photometric, and spectroscopic (redshift) data. In this paper, we consider only isothermal models; however, our analysis can be easily extended to non-isothermal radial mass profiles.

This paper is organized as follows. In section 2, we describe the models that we used to investigate four systems. In section 3, we show how we applied the models to four systems and give the results. We finally discuss the results and give conclusions in section 4. The linear method that we used is presented in Appendix 1.

2. Lens Model and Method

2.1. Fundamental Equations of Gravitational Lensing

A source at \mathbf{x}_s and an image i at \mathbf{x}_i are related through the lens equation,

$$\mathbf{x}_i - \mathbf{x}_s = \nabla \psi(\mathbf{x}_i), \quad (1)$$

where $\psi(\mathbf{x})$ is the projected lens potential. Thus, the magnification factor is given by

$$\mu(\mathbf{x}_i) = \left[\det \left(\frac{\partial \mathbf{x}_s}{\partial \mathbf{x}_i} \right) \right]^{-1}. \quad (2)$$

We can also calculate the equation of the relative time delay between image i and j using

$$\Delta t_{ij} = \frac{1 + z_d}{c} \frac{D_d D_s}{D_{ds}} \left[\frac{1}{2} \Delta \mathbf{x}_i^2 - \frac{1}{2} \Delta \mathbf{x}_j^2 - \psi(\mathbf{x}_i) + \psi(\mathbf{x}_j) \right], \quad (3)$$

where z_d is the redshift of the lens object and c is the speed of light; D_d , D_s , and D_{ds} are the angular diameter distances to the lens, to the source, and from the lens to the source, respectively; $\Delta \mathbf{x}_i = \mathbf{x}_i - \mathbf{x}_s$ (Schneider et al. 1992). The two-dimensional Poisson equation relates the dimensionless density distribution $\kappa(\mathbf{x})$ to the lens potential as

$$\nabla^2 \psi(\mathbf{x}) = 2\kappa(\mathbf{x}). \quad (4)$$

2.2. Lens Model

For the potential of the primary lens galaxy, we apply the singular isothermal elliptical density (SIED) model and/or the power-law Fourier potential (PLF; Oguri, Kawano 2003; Evans, Witt 2003) model. The former model may be called the ‘‘standard’’ model in the sense that it is widely used in the mass modeling of a lens galaxy. The two-dimensional density profile of SIED is given, in the Cartesian coordinates (x, y) centered on the primary lens galaxy, as

$$\kappa_{\text{galaxy}}(\mathbf{x}) = b(x^2 + y^2/q^2)^{-1/2}, \quad (5)$$

where b is the mass parameter that characterizes the Einstein radius and q is the axis ratio. The ellipticity, e , is given by $1 - q$. We used the latter model, PLF, to investigate the contribution of multipoles, particularly an $m = 3$ multipole, which is neglected in usual lens modelings of lens systems. In addition, this model has an advantage that we can apply a linear method (Appendix 1). The lens potential of the power-law Fourier model is given by

$$\psi_{\text{galaxy}} = r^\beta F(\theta), \quad (6)$$

where a Fourier expansion of the angular function $F(\theta)$ is

$$F(\theta) = a_0 + \sum_{m=1}^{\infty} (a_m \cos m\theta + b_m \sin m\theta) \quad (7)$$

$$= a_0 + \sum_{m=1}^{\infty} A_m \cos\{m(\theta - \theta_m)\}, \quad (8)$$

in polar coordinates (r, θ) . The variables $A_m = (a_m^2 + b_m^2)^{1/2}$ and θ_m are the amplitude and the position angle of the multipole, respectively. In the present work, we considered only the case of $\beta = 1$, which has a similar radial profile as in SIED, while the parameter β can take values between 0 (point mass) and 2 (mass sheet).

While the influence of the galaxy group which embeds the primary lens galaxy should be taken into account (e.g., Keeton et al. 1997; Witt et al. 2000), detailed information on the density distribution of the group is uncertain in most cases. The potential near the lens galaxies is often described by a singular isothermal sphere (SIS) or the potential expanded around the center of the lens galaxy (Kochanek 1991; Bernstein, Fischer 1999 Keeton et al. 2000) as

$$\psi_{\text{ex}} = \psi_0 + \boldsymbol{\psi}_1 \cdot \mathbf{x} + r^2 \left[\frac{1}{2} \kappa_0 + \frac{1}{2} \gamma \cos 2(\theta - \theta_\gamma) \right] + r^3 \left[\frac{1}{4} \sigma \sin(\theta - \theta_\sigma) - \frac{1}{6} \delta \sin 3(\theta - \theta_\delta) \right] + \mathcal{O}(r^4). \quad (9)$$

The first three terms cannot be fully constrained by observables, because of the lens degeneracies (Falco et al. 1985; Gorenstein et al. 1988; Saha 2000). Thus, one usually uses an external shear (XS),

$$\psi_{\text{xs}} = \frac{\gamma}{2} r^2 \cos 2(\theta - \theta_\gamma) = \frac{\gamma_1}{2} r^2 \cos 2\theta + \frac{\gamma_2}{2} r^2 \sin 2\theta, \quad (10)$$

where $\gamma_1 = \gamma \cos 2\theta_\gamma$ and $\gamma_2 = \gamma \sin 2\theta_\gamma$. In the present work, we also added the terms of third order (r^3) to the lens potential in a similar way of e.g., Bernstein and Fischer (1999) enforcing $\delta = -(3/2)\sigma$ and $\theta_\delta = \theta_\sigma$ (as for a singular isothermal group). In this case, the explicit expression of the additional potential (X3) is

$$\psi_{\text{x3}} = \frac{r^3}{4} \sigma [\sin(\theta - \theta_\sigma) + \sin 3(\theta - \theta_\sigma)]. \quad (11)$$

In summary, we used SIS, SIED, and PLF models for the primary lens galaxy, and XS, SIS, or (XS + X3) models for the group.

2.3. Method

We used image positions and flux ratios as constraints on the lens models. The relative time delays between images were used not only for determining the Hubble constant, but also for additional constraints on the lens models. The number of constraints was more than ten for a quadruple lens system, while the typical number of model parameters is equal to or more than seven. The goodness of fit was determined by χ^2 statistics based on the image positions, the flux ratios, and the relative time delays:

$$\chi_{\text{pos}}^2 = \sum_i \frac{|\mathbf{x}_i - \mathbf{x}_i^{(\text{model})}|^2}{\sigma_{xi}^2}, \quad (12)$$

$$\chi_{\text{flux}}^2 = \sum_{i < j} \frac{(f_{ij} - f_{ij}^{(\text{model})})^2}{\sigma_{fij}^2}, \quad (13)$$

$$\chi_{\text{time}}^2 = \sum_{i < j} \frac{(\Delta t_{ij} - \Delta t_{ij}^{(\text{model})})^2}{\sigma_{tij}^2}. \quad (14)$$

In the above equations, \mathbf{x}_i are the observed image positions, f_{ij} are the observed flux ratios, and Δt_{ij} are the observed relative time delays. The suffix “(model)” indicates the model predictions for each observable. The uncertainties in the observables are represented by σ_{xi} , σ_{fij} , and σ_{tij} . We minimized the total chi-square, $\chi_{\text{total}}^2 = \chi_{\text{pos}}^2 + \chi_{\text{flux}}^2 + \chi_{\text{time}}^2$ (Press et al. 1992), to obtain the best-fit parameters, \mathbf{u}_{best} . In this fitting, (i) we solved non-linear lens equations to derive the model predictions for the image positions, (ii) calculated the relative time delays and the flux ratios from the predicted image positions and the model parameters, and (iii) evaluated and minimized χ_{total}^2 . Finally, we evaluated the reduced chi-square, $\chi_{\text{total}}^2/N_{\text{dof}}$, where N_{dof} is the number of degrees of freedom. In the case of the PLF model, the χ^2 minimization was significantly simplified because of the linearity of the equations (see Appendix 1).

3. Results

About 80 gravitational-lens systems have been reported so far. One third of them are quadruple-lens systems, and the rest are double-lens systems. However, we considered only quadruple lens systems, because more than six observables are typically needed to strongly constrain lens models. Specifically, we analyzed the systems PG 1115+080 (Weymann et al. 1980), B1422+231 (Patnaik et al. 1992), B0712+472 (Jackson et al. 1998), and B2045+265 (Fassnacht et al. 1999). We adopted a flat lambda-dominated universe with $(\Omega_0, \Omega_\Lambda) = (0.3, 0.7)$, where Ω_0 is the density parameter of matter and Ω_Λ is the dimensionless cosmological constant. The Hubble constant in units of $100 \text{ km s}^{-1} \text{ Mpc}^{-1}$ is denoted by h , as usual.

3.1. Data

The positions and fluxes of most of the gravitationally lensed images are relatively well constrained within 10 mas and about five percent uncertainties, respectively, while measuring time delays from light curves are very difficult. For most of the systems, we used the data of the image positions and the fluxes by the CfA/Arizona Space Telescope Lens Survey¹ (CASTLES; Falco et al. 1999), and for some of the systems the data was taken from the papers cited below. The uncertainties of the flux ratios were slightly broadened (see below) to account for possible systematics, such as possible microlensing (e.g., Mao, Schneider 1998), extinction, and quasar variability during a time delay.

The system PG 1115+080 is a QSO ($z_s = 1.72$) gravitationally lensed by an early-type galaxy of $z_d = 0.31$, which looks very spherical (Keeton et al. 1998; Iwamuro et al. 2000). The lens galaxy belongs to a group of galaxies. The QSO images consist of four components (fold-type) with the maximum angular separation of $2''.32$. In order to constrain models, we used the CASTLES data of the image positions and the fluxes, and Barkana (1997)’s analysis of the time delays. The flux uncertainties were broadened to 20%.

¹ (<http://cfa-www.harvard.edu/castles/>).

The second system, B1422+231, that we analyzed is known as a system with possible substructure microlensing (Mao, Schneider 1998; Keeton 2001; Chiba 2002; Bradač et al. 2002; Keeton et al. 2003; Kochanek, Dalal 2003). The elongated galaxy ($z_d = 0.34$) associated with a poor group gravitationally lenses a QSO ($z_s = 3.62$), and leads to a cusp-type four-imaged system. The ellipticity, e , of the galaxy is 0.27 ± 0.13 (Impey et al. 1996). There are radio data of this system (Patnaik et al. 1992, 1999), having uncertainties of $50 \mu\text{as}$ for QSO images and a few percents for their fluxes. Some other observational properties, such as the effects of the Lyman α (Bechtold, Yee 1995; Petry et al. 1998) and the variability (Yee, Bechtold 1996; Koopmans et al. 2003), have been observed. We used the data of Patnaik et al. (1999), assuming flux uncertainties of 5%.

We also investigated an interesting system B0712+472 (Jackson et al. 1998). The redshifts of the elongated primary lens galaxy and the source QSO are 0.41 and 1.34, respectively. Interestingly, the primary lens galaxy is not associated with a group of galaxies, but a foreground group with a mean redshifts of 0.29 are overlapped (Fassnacht, Lubin 2002). The light distribution of the galaxy is very elongated with an ellipticity of between 0.4 and 0.5. The positions of the QSO and the galaxy images that we used were from Jackson et al. (1998) and CASTLES, respectively. For the fluxes, radio data of Jackson et al. (1998) were used, assuming 20% uncertainties.

The system B2045+265 was discovered by a radio survey of the Cosmic Lens All-Sky Survey (CLASS). Five radio components were clearly observed (Fassnacht et al. 1999). The four components are the lensed QSO ($z_s = 1.28$) and another component is the radio core of the primary lens galaxy ($z_d = 0.87$), which is associated with a compact group of galaxies. The optical spectrum of the galaxy is similar to that of nearby Sa galaxies. We used the data of CASTLES for the galaxy and those of Fassnacht et al. (1999) for the QSO. The flux uncertainties were assumed to be 20% uncertainties.

3.2. Implications from Models

Table 1 gives the results of PG 1115+080 with typical models that we described in previous section. Some models [($m = 3$)+XS, SIS+(XS+X3), and SIS+SIS] well reproduce the image positions, the flux ratios, and the relative time delays. While most previous authors applied a SIED+XS or a SIED+SIS, our results clearly imply that the lens requires the term $\cos 3\theta$, which might be a component of the primary lens galaxy ($m = 3$ multipole), or be that of the external perturbation of the group (X3). A very small amplitude ($A_3/a_0 \approx 0.002$) of the $m = 3$ multipole of the galaxy is consistent with the galaxy light distribution, which is very spherical. While some of the models including only XS as the external perturbation fail to reproduce the observables, inclusion of the contribution from the group represented by SIS and XS+X3 always gives a better fit, i.e., an X3 perturbation is important to improve the fit. The best fit of the angles in the external perturbation is $\theta_\gamma = -115^\circ$ and $\theta_\sigma = -160^\circ$. These angles are consistent with optical (Impey et al. 1998) and X-ray (Grant et al. 2003) observations of the group. Therefore, we conclude that there is a degeneracy between an $m = 3$ multipole of the lens galaxy and an X3 perturbation of the group in this lens system, possibly because the galaxy is very spherical and the external shear is small. The mass distribution of the galaxy might be spherical and the ellipticity of the galaxy might be *unnecessary*. Schechter et al. (1997) also used the model of a SIS+SIS, but they did not allow the galaxy position to vary. Allowing a variable galaxy position is essential.

The results of B1422+231 are given in table 2. While the SIED+XS and even the SIED+SIS cannot reproduce the observables of the system, particularly the flux ratios, including the perturbation of X3 significantly reduced the χ^2/N_{dof} to less than 2 [see the (SIED+ $m = 3$)+XS model]. The fact that the angles of the external perturbations are somewhat strange, $|\theta_\gamma - \theta_\sigma| = |134^\circ - 63^\circ| = 71^\circ$, implies that the structure of the group is not so simple as SIS. Recent X-ray observations (Grant et al. 2003) support this interpretation. Moreover, the direction of the σ perturbation in our modeling [equation (9)] coincides with the direction of the gradient of the group density distribution. Note that a part of the large misalignment of the external perturbations (γ and σ) may arise from limiting the amplitudes and the directions of the r^3 perturbation [equation (11)]. Since the system was well-fitted

Table 1. Results of PG 1115+080.

| Model | χ^2/N_{dof} | Best-fit parameters | Note |
|----------------|-------------------------|---|----------------|
| SIED | 537.9/8 | $e = 0.32, \theta_e = 66^\circ$ | |
| SIS+XS | 257.0/8 | $\gamma = 0.11, \theta_\gamma = -115^\circ$ | |
| SIED+XS | (27.4 + 1.5 + 1.8)/6 | $e = 0.18, \theta_e = 89^\circ$ $\gamma = 0.09, \theta_\gamma = -132^\circ$ | |
| SIS+(XS+X3) | (0.6 + 2.9 + 0.3)/6 | $\gamma = 0.12, \theta_\gamma = -115^\circ$ $\sigma = 0.008, \theta_\sigma = -160^\circ$ | Acceptable fit |
| SIS+SIS | (2.6 + 2.7 + 0.2)/7 | $r_{\text{group}} = 12''.4, \theta_{\text{group}} = -116^\circ$ | Acceptable fit |
| ($m = 2$)+XS | (27.8 + 1.5 + 1.7)/6 | $\gamma = 0.11, \theta_\gamma = -129^\circ$ $A_2/a_0 = 0.03, \theta_2 = 6^\circ$ | |
| ($m = 3$)+XS | (1.0 + 3.3 + 0.7)/6 | $\gamma = 0.12, \theta_\gamma = -115^\circ$ $A_3/a_0 = 0.002, \theta_3 = -14^\circ$ | Acceptable fit |

Notes. The χ^2 is the total chi-square, $\chi_{\text{pos}}^2 + \chi_{\text{flux}}^2 + \chi_{\text{time}}^2$. Model denotes the used potential of galaxy+group. The position of the group center is ($r_{\text{group}}, \theta_{\text{group}}$).

Table 2. Results of B1422+231.

| Model | χ^2/N_{dof} | Best-fit parameters | Note |
|-----------------|-------------------------|---|-----------------|
| SIED+XS | (2.5 + 12.2)/4 | $e = 0.28, \theta_e = -56^\circ$ $\gamma = 0.16, \theta_\gamma = 127^\circ$ | |
| SIED+SIS | (1.5 + 9.0)/3 | $e = 0.22, \theta_e = -58^\circ$ $r_{\text{group}} = 9''.5, \theta_{\text{group}} = 128^\circ$ | |
| SIED+(XS+X3) | (0.1 + 3.8)/2 | $e = 0.25, \theta_e = -59^\circ$ $\gamma = 0.20, \theta_\gamma = 134^\circ$ $\sigma = 0.02, \theta_\sigma = 63^\circ$ | Acceptable fit |
| [SIED+(m=3)]+XS | (0.1 + 6.1)/2 | $e = 0.29, \theta_e = -55^\circ$ $\gamma = 0.17, \theta_\gamma = 129^\circ$ $A_3/a_0 = 0.007, \theta_3 = -16^\circ$ | |
| (m=3)+XS | 781.8/4 | $\gamma = 0.21, \theta_\gamma = 124^\circ$ $A_3/a_0 = 0.01, \theta_3 = -18^\circ$ | Too large A_3 |

Notes. The χ^2 is the total chi-square, $\chi_{\text{pos}}^2 + \chi_{\text{flux}}^2$. Model denotes the used potential of galaxy+group.

Table 3. Results of B0712+472.

| Model | χ^2/N_{dof} | Best-fit parameters | Note |
|-----------------|-------------------------|---|-----------------|
| SIED | (33.5 + 54.6)/6 | $e = 0.33, \theta_e = 50^\circ$ | |
| SIS+XS | (53.2 + 86.8)/6 | $\gamma = 0.12, \theta_\gamma = 49^\circ$ | |
| SIED+XS | (10.1 + 3.0)/4 | $e = 0.73, \theta_e = 56^\circ$ $\gamma = 0.33, \theta_\gamma = -34^\circ$ | |
| SIED+SIS | (9.3 + 4.9)/3 | $e = 0.61, \theta_e = 55^\circ$ $r_{\text{group}} = 6''.0, \theta_{\text{group}} = 152^\circ$ | |
| SIED+(XS+X3) | (2.5 + 4.8)/2 | $e = 0.69, \theta_e = 56^\circ$ $\gamma = 0.32, \theta_\gamma = -43^\circ$ $\sigma = 0.19, \theta_\sigma = 123^\circ$ | |
| [SIED+(m=3)]+XS | (3.9 + 0.7)/2 | $e = 0.63, \theta_e = 54^\circ$ $\gamma = 0.22, \theta_\gamma = -39^\circ$ $A_3/a_0 = 0.01, \theta_3 = 37^\circ$ | Too large A_3 |

Notes. The χ^2 is the total chi-square, $\chi_{\text{pos}}^2 + \chi_{\text{flux}}^2$. Model denotes the used potential of galaxy+group.

with 5% flux uncertainties, it may be unnecessary to consider microlensing by substructure, or other compact structures, for this system, which supports the analysis of Keeton, Gaudi, and Petters (2003) using the cusp relation.

We also show results of B0712+472 in table 3. In this system, it does not seem that fitting by the SIED+XS model was significantly improved by including other additional terms, such as an $m = 3$ multipole of the galaxy and X3 terms of the group. Therefore, it may be better to consider the existence of substructure(s) in this galaxy. However, we note that the curves of the flux ratios are variable, and perhaps further observational studies are needed (see Koopmans et al. 2003). Another interesting result is that both the ellipticity of the primary lens galaxy and the amplitude of the external shear of the foreground group are large in a *two*-shear model, such as SIED+XS. This is in marked contrast with the *one*-shear model studied so far (Keeton et al. 1998; Jackson et al. 1998; Fassnacht, Lubin 2002) in which the ellipticity of the light is larger than that of the mass and the external shear is very small ($\gamma < 0.1$). We believe that the results with ellipticity plus external shear are more realistic, since the two shears are in good agreement with that of observed light. The conflict between the two can be easily understood by the fact $|\theta_e - \theta_\gamma| \approx 90^\circ$, where θ_e is the angle of the mass ellipticity. Here, we roughly represent the potential of the SIED as the PLF to $m = 2$,

$$\psi_{\text{SIED}} \approx r [a_0 + A_e \cos 2(\theta - \theta_e)], \quad (15)$$

where A_e is the amplitude of the mass ellipticity. Their contribution to the lens potential is approximately expressed (without r dependences) as $A_e \cos 2(\theta - \theta_e) + (\gamma/2) \cos 2(\theta - \theta_\gamma) = A_e \cos 2(\theta - \theta_e) + (\gamma/2) \cos 2(\theta - \theta_e - 90^\circ) = (A_e - \gamma/2) \cos 2(\theta - \theta_e)$. Therefore, while two amplitudes, A_e and γ , of ellipticity-only and external shear-only models are small, those of realistic ellipticity plus external shear model are large.

In the case of B2045+265, all models that we considered could not reproduce the observables well (table 4), particularly the flux ratios. Some models reduce the χ^2 , but we find that they are not physical. However, the system shows very large (up to

Table 4. Results of B2045 + 265.

| Model | χ^2/N_{dof} | Best-fit parameters | Note |
|-----------------|-------------------------|---|------------|
| SIED+XS | 481.1/4 | $e = 0.19, \theta_e = -70^\circ$ $\gamma = 0.10, \theta_\gamma = -69^\circ$ | |
| SIED+SIS | (16.0 + 48.0)/3 | $r_{\text{sis}} = 1''.5, \theta_{\text{sis}} = -66^\circ$ | Not smooth |
| SIED+(XS+X3) | (2.3 + 15.2)/2 | $e = 0.81, \theta_e = -68^\circ$ $\gamma = 0.66, \theta_\gamma = 21^\circ$ $\sigma = 0.21, \theta_\sigma = 160^\circ$ | |
| [SIED+(m=3)]+XS | 311.4/2 | $e = 0.37, \theta_e = 24^\circ$ $\gamma = 0.22, \theta_\gamma = -67^\circ$ $A_3/a_0 = 0.03, \theta_3 = -70^\circ$ | |

Notes. The χ^2 is the total chi-square, $\chi_{\text{pos}}^2 + \chi_{\text{flux}}^2$. Model denotes the used potential of galaxy+group.

$\sim 40\%$) extrinsic variations of fluxes (Koopmans et al. 2003) on time scales of several months, depending on the frequency (Fassnacht et al. 1999). Therefore, it may be premature to conclude that this system shows substructure lensing, given that the nature of their variabilities still remains to be understood. One possibility is the Galactic scintillation as Koopmans et al. (2003) indicated, and another one is anomalous gravitational lensing by the inner structure of the primary lens galaxy.

4. Conclusion

We investigated four quadruple gravitational lens systems (PG 1115+080, B1422+231, B0712+472, and B2045+265) using mass models of SIED or PLF as well as external perturbations described by SIS, or several truncations of the expansion of the external perturbation. We performed χ^2 fittings with all of the models presented in section 2 in order to study the contribution of terms that are usually not included in mass modelings, such as $m = 3$ multipoles of primary lens galaxy and next-order external perturbations.

We have found that the $m = 3$ multipoles and/or X3 external perturbation significantly reduce the χ^2 in PG 1115+080 and B1422+231. In PG 1115+080, not only the external perturbation of the r^3 order (X3), but also an internal $m = 3$ multipole, reduces the χ^2 to statistically acceptable values, but the ellipticity of the galaxy does not. Their amplitudes and directions seem to be physical, comparing the results with optical and X-ray observations of the galaxy and the group (Impey et al. 1998; Grant et al. 2003); in a $(m = 3)$ +XS model the ratio $A_3/a_0 \approx 0.002$ is small enough to reproduce the observed very spherical galaxy, and in a SIS+(XS+X3) model the ratio $\sigma/\gamma \approx 0.1$ and the angles $\theta_\gamma = -115^\circ$ and $\theta_\sigma = -160^\circ$ can be expected from the positions of the member galaxies and the X-ray brightness contours. A SIS group also provides an acceptable fit. A significant (but small) $m = 3$ galaxy multipole might be induced by interactions with the member galaxies. Regarding B1422+231, several authors concluded that the ‘‘anomalous’’ flux ratios reflected the existence of substructure lensing (e.g., Mao, Schneider 1998; Chiba 2002; Bradač et al. 2002; Kochanek, Dalal 2003). However, Keeton, Gaudi, and Petters (2003) found that the cusp relation does not reveal a significant anomaly in the system. In fact, our analysis has revealed that a SIED+(XS+X3) model without substructure reproduces the fluxes within 5% errors. In addition, the X-ray brightness contours (figure 2 of Grant et al. 2003) imply that the direction of the gradient of the group mass is $\approx 90^\circ$ – 180° , and that the shapes of the contours are significantly deformed, which are consistent with the results of SIED+(XS+X3) model. In the other systems, B0712+472 and B2045+265, the contribution of the $m = 3$ multipoles and X3 external perturbations to the lens potentials do not significantly improve the model fitting. In B0712+472, however, we find that the ellipticity and shear are well misaligned, $\theta_e \approx 56^\circ$ and $\theta_\gamma \approx 146^\circ$, and that the result is very consistent with the lens galaxy and the foreground group observed by Fassnacht and Lubin (2002). Therefore, the models including only ellipticity or shear may underestimate these (see subsection 3.2). The relatively large shear may arise from the elongated shape of the group.

In summary, the terms of an $m = 3$ multipole of the primary lens galaxy and of an X3 external perturbation, which are often neglected in strong lens analyses, sometimes improve the fit significantly. The contribution of the group particularly needs to be studied in more detail. Simple models (in particular one-shear models) may often mislead us.

This work is supported by a Grant-in-Aid for JSPS Fellows.

Appendix 1. The Linear Method

The linear method that we used in this work is as follows. First, we choose a model of Fourier expansion of $F(\theta)$ for a fixed value of β . Second, for the observed image positions and the relative time delays, we solve a set of linear equations [equations (1) and (3)]

$$A\mathbf{u} = \mathbf{v}, \tag{A1}$$

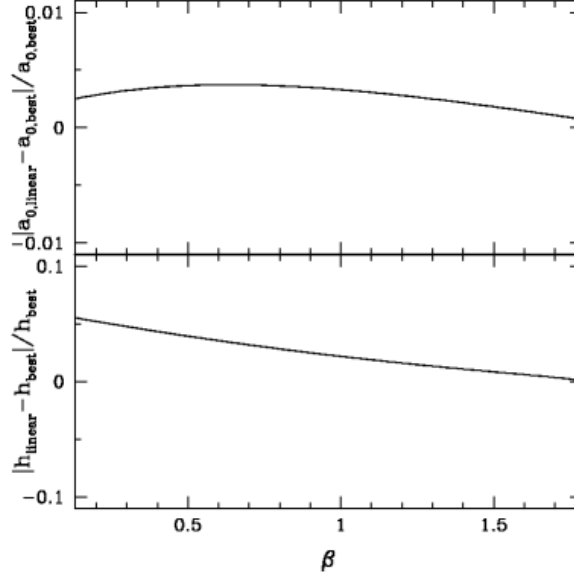


Fig. 1. The normalized deviations of a_0 and h of $\mathbf{u}_{\text{linear}}$ from those of \mathbf{u}_{best} in the case of PG 1115+080. We use the time delays derived by Barkana (1997). The errors of a_0 and h of \mathbf{u}_{best} are 0.01 and 0.1, respectively. The isothermal model corresponds to $\beta = 1$.

where $N \times M$ matrix A and N dimensional vector \mathbf{v} are functions of observable quantities, such as the image positions and the relative time delays, to obtain an initial guess of the parameters $\mathbf{u}_{\text{linear}}$ from which we start to search a minimum of the χ^2 . Explicitly, the matrix A is expressed as

$$\begin{pmatrix} a_{11} & a_{21} & \alpha_{01} & \alpha_{m1} & \beta_{m1} & \gamma_{11} & \gamma_{21} & 0 \\ a'_{11} & a'_{21} & 0 & \alpha'_{m1} & \beta'_{m1} & \gamma'_{11} & \gamma'_{21} & 0 \\ \vdots & 0 \\ \Delta x_{ij} & \Delta y_{ij} & \hat{\alpha}_{0ij} & \hat{\alpha}_{mij} & \hat{\beta}_{mij} & \hat{\gamma}_{1ij} & \hat{\gamma}_{2ij} & T \\ \vdots & \vdots \end{pmatrix}, \quad (\text{A2})$$

where $a_{1i} = \cos\theta_i$, $a_{2i} = \sin\theta_i$, $\alpha_{0i} = \beta r_i^{\beta-1}$, $\alpha_{mi} = \beta r_i^{\beta-1} \cos m\theta_i$, $\beta_{mi} = \beta r_i^{\beta-1} \sin m\theta_i$, $\gamma_{1i} = r_i \cos 2\theta_i$, $\gamma_{2i} = r_i \sin 2\theta_i$, $a'_{1i} = -\sin\theta_i$, $a'_{2i} = \cos\theta_i$, $\alpha'_{mi} = -m r_i^{\beta-1} \sin m\theta_i$, $\beta'_{mi} = m r_i^{\beta-1} \cos m\theta_i$, $\gamma'_{1i} = -r_i \sin 2\theta_i$, $\gamma'_{2i} = r_i \cos 2\theta_i$, $\Delta x_{ij} = x_i - x_j$, $\Delta y_{ij} = y_i - y_j$, $\hat{\alpha}_{0ij} = r_i^\beta - r_j^\beta$, $\hat{\alpha}_{mij} = r_i^\beta \cos m\theta_i - r_j^\beta \cos m\theta_j$, $\hat{\beta}_{mij} = r_i^\beta \sin m\theta_i - r_j^\beta \sin m\theta_j$, $\hat{\gamma}_{1ij} = (1/2)(r_i^2 \cos 2\theta_i - r_j^2 \cos 2\theta_j)$, $\hat{\gamma}_{2ij} = (1/2)(r_i^2 \sin 2\theta_i - r_j^2 \sin 2\theta_j)$, and $T = D^{-1} \Delta t_{ij}$ ($[1 + z_d] D_d D_s / c D_{ds} \equiv D h^{-1}$), respectively. The elements of $(2i - 1)$ -th and $(2i)$ -th lines are from the lens equations of an image i . The elements of lines that are below $(2n)$ -th line are ones of observed time delay for an n imaged system. The vector \mathbf{u} is given as

$$\mathbf{u}^T = (x_s, y_s, a_0, a_m, b_m, \gamma_1, \gamma_2, h). \quad (\text{A3})$$

Finally, the vector \mathbf{v} is expressed as

$$\mathbf{v}^T = \left(r_1, 0, \dots, \frac{1}{2}(r_i^2 - r_j^2), \dots \right). \quad (\text{A4})$$

Usually, the number of linear equations N (at most 11 for a quadruple lens system) should be equal or larger than that of linear model parameters M . However, we can truncate some of the linear equations so that the number of linear equations is the same as that of the parameters, $N = M$. Thus, the parameters derived from the linear method are $\mathbf{u}_{\text{linear}} = A^{-1} \mathbf{v}$. We find that this initial guess is close to the actual minimum of the χ^2 , provided that the observed values have sufficiently small errors. Especially, the Hubble constant, one of the most interesting parameters cosmologically, of $\mathbf{u}_{\text{linear}}$ coincides with that of \mathbf{u}_{best} within 1σ uncertainties. Figure 1 shows the result of the linear method in PG 1115+080, the normalized deviations of a_0 and h of $\mathbf{u}_{\text{linear}}$ from those of \mathbf{u}_{best} within 1σ errors as a function of β (0.01 for a_0 and 0.1 for h). Therefore, this method is useful enough to estimate the Hubble constant accurately and quickly without solving nonlinear equations.

Our linear method is complementary to that of Evans and Witt (2003) in the sense that our method is applicable to arbitrary values of β and can derive the external shear as well (the essence of theirs is the fact that for $\beta = 1$ the magnification factor is expressed as a linear equation with respect to the model parameter,

$$\mu(\mathbf{x}) = \left\{ (1 - \kappa)^2 - \left[|\gamma|^2 + \kappa^2 - \frac{4\kappa}{r^2} \psi_{\text{ex}} \right] \right\}^{-1} \quad (\text{A5})$$

$$= \left\{ 1 - 2\kappa(1 - \gamma_1 \cos 2\theta - \gamma_2 \sin 2\theta) - |\gamma|^2 \right\}^{-1}, \quad (\text{A6})$$

when the external shear is assumed). The two methods can be combined in the case of $\beta = 1$; first one estimates the external shear with the former and then applies the latter to the considered system in order to reproduce the flux ratios *without* assuming the external shear. However, this combined method sometimes suffers from results of unphysical galaxy shapes, such as cross-like ones.

References

- Barkana, R. 1997, ApJ, 489, 21
 Bechtold, J., & Yee, H. K. C. 1995, AJ, 110, 1984
 Bernstein, G., & Fischer, P. 1999, AJ, 118, 14
 Bradač, M., Schneider, P., Steinmetz, M., Lombardi, M., King, L. J., & Porcas, R. 2002, A&A, 388, 373
 Chiba, M. 2002, ApJ, 565, 17
 Chiba, T., & Takahashi, R. 2002, Prog. Theor. Phys., 107, 625
 Courbin, F., Magain, P., Keeton, C. R., Kochanek, C. S., Vandierriest, C., Jaunsen, A. O., & Hjorth, J. 1997, A&A, 324, L1
 Evans, N. W., & Witt, H. J. 2003, MNRAS, 345, 1351
 Falco, E. E., et al. 1999, in ASP Conf. Ser. 237, Gravitational Lensing: Recent Progress and Future Goals, ed. T. G. Brainerd & C. S. Kochanek (San Francisco: ASP), 25
 Falco, E. E., Gorenstein, M. V., & Shapiro, I. I. 1985, ApJ, 289, L1
 Fassnacht, C. D., et al. 1999, AJ, 117, 658
 Fassnacht, C. D., & Lubin, L. M. 2002, AJ, 123, 627
 Gorenstein, M. V., Falco, E. E., & Shapiro, I. I. 1988, ApJ, 327, 693
 Grant, C. E., Bautz, M. W., Chartas, G., & Garmire, G. P. 2003, ApJ, submitted (astro-ph/0305137)
 Impey, C. D., Falco, E. E., Kochanek, C. S., Lehár, J., McLeod, B. A., Rix, H.-W., Peng, C. Y., & Keeton, C. R. 1998, ApJ, 509, 551
 Impey, C. D., Foltz, C. B., Petry, C. E., Browne, I. W. A., & Patnaik, A. R. 1996, ApJ, 462, L53
 Iwamuro, F., et al. 2000, PASJ, 52, 25
 Jackson, N., et al. 1998, MNRAS, 296, 483
 Keeton, C. R. 2001, ApJ, submitted (astro-ph/0111595)
 Keeton, C. R., et al. 2000, ApJ, 542, 74
 Keeton, C. R., Gaudi, B. S., & Petters, A. O. 2003, ApJ, 598, 138
 Keeton, C. R., & Kochanek, C. S. 1997, ApJ, 487, 42
 Keeton, C. R., Kochanek, C. S., & Falco, E. E. 1998, ApJ, 509, 561
 Keeton, C. R., Kochanek, C. S., & Seljak, U. 1997, ApJ, 482, 604
 Kochanek, C. S. 1991, ApJ, 382, 58
 Kochanek, C. S., & Dalal, N. 2003, ApJ, submitted (astro-ph/0302036)
 Koopmans, L. V. E., et al. 2003, ApJ, 595, 712
 Mao, S., & Schneider, P. 1998, MNRAS, 295, 587
 Oguri, M., & Kawano, Y. 2003, MNRAS, 338, L25
 Oguri, M., Taruya, A., Suto, Y., & Turner, E. L. 2002, ApJ, 568, 488
 Patnaik, A. R., Browne, I. W. A., Walsh, D., Chaffee, F. H., & Foltz, C. B. 1992, MNRAS, 259, 1P
 Patnaik, A. R., Kembball, A. J., Porcas, R. W., & Garrett, M. A. 1999, MNRAS, 307, L1
 Petry, C. E., Impey, C. D., & Foltz, C. B. 1998, ApJ, 494, 60
 Press, W. H., Teukolsky, S. A., Vetterling, W. T., & Flannery, B. P. 1992, Numerical Recipes in Fortran (Cambridge: Cambridge Univ. Press)
 Refsdal, S. 1964, MNRAS, 128, 307
 Saha, P. 2000, AJ, 120, 1654
 Schechter, P. L., et al. 1997, ApJ, 475, L85
 Schneider, P., Ehlers, J., & Falco, E. E. 1992, Gravitational Lenses (New York: Springer)
 Walsh, D., Carswell, R. F., & Weymann, R. J. 1979, Nature, 279, 381
 Wambsgans, J., & Paczyński, B. 1994, AJ, 108, 1156
 Weymann, R. J., et al. 1980, Nature, 285, 641
 Witt, H. J., Mao, S., & Keeton, C. R. 2000, ApJ, 544, 98
 Wucknitz, O. 2002, MNRAS, 332, 951
 Wucknitz, O., & Refsdal, S. 1999, (astro-ph/9909291)
 Yee, H. K. C., & Bechtold, J. 1996, AJ, 111, 1007